Acc. Chem. Res. **1998,** *31,* 755−763

Protein Folding Triggered by Electron Transfer

JASON R. TELFORD,
PERNILLA WITTUNG-STAFSHEDE,
HARRY B. GRAY,* AND JAY R. WINKLER*

Beckman Institute, California Institute of Technology, Pasadena, California 91125

Received January 16, 1998

Background

Proteins do not fold by randomly searching a large number of nearly degenerate configurations; instead, an ensemble of unfolded molecules must traverse a complicated energy landscape to reach a thermodynamically stable structure.[1−5] The fastest nuclear motions in proteins, rotations about single bonds, occur on the picosecond time scale and accompany both secondary- and tertiary-structure-forming processes.[6] Short segments of secondary structure (e.g., α-helices) can be formed in nanoseconds,[7] whereas the large-scale, collective motions associated with the development of tertiary structure fall in the microsecond to millisecond range. Misfolded structures or traps are frequently encountered in folding processes; escape from these traps (e.g., proline isomerization) can take seconds or even minutes.[8] Understanding the key events in folding and identifying any partially folded intermediates are major goals of theoretical[1−5,9,10] and experimental[11−18] work.

Rapid mixing techniques, including stopped-flow kinetic spectroscopy and pulsed deuterium-exchange NMR, have been employed to gather the vast majority of available experimental data on folding kinetics.[19−25] Pulsed deuterium-exchange experiments, in particular, have been extremely informative, yielding residue-specific information.[12,13,17,22,26,27] In many rapid-mixing investigations of folding, however, submillisecond "burst phases" have been observed.[19,28−32] It has been speculated that some secondary-structure formation and a collapse to a compact denatured state (molten globule) occur during this burst, but faster methods are necessary to resolve this issue.[16,19,32]

Folding Triggers

A basic requirement for experimental investigations of kinetics is some means of triggering the folding (or unfolding) process.[18] New approaches are necessary to break the millisecond time barrier and resolve the events occurring during the burst phase. Recent technical advances are pushing the dead time for rapid mixing down to ∼100 μs.[33−37] Conventional temperature jump has been used to examine the refolding of cold-denatured proteins.[38,39] Laser-initiated temperature jumps, capable of subnanosecond time resolution, have been employed by several groups in studies of the folding and unfolding dynamics of peptides and proteins.[7,40−44]

Lasers also can trigger protein folding by initiating a photochemical reaction that shifts the folded/unfolded equilibrium. The first study of this type examined the folding of ferrocytochrome *c* (Fe^{II}-cyt *c*).[11] Carbonmonoxy ferrocytochrome *c* ((CO)Fe^{II}-cyt *c*) is less stable toward denaturants than the native protein. The folding of Fe^{II}-cyt_U *c* in this investigation was triggered by laser-initiated carbon monoxide dissociation from the heme in less than 10 ns.[11] Since the experiments were performed under an atmosphere of carbon monoxide, rebinding of CO (∼1 ms) prevented complete folding of the protein. Our photochemical approach is based on the oxidation-state dependence of the folding stabilities of redox-active proteins.[45]

Redox-Coupled Folding

The formal potentials for redox cofactors in the interiors of proteins often are shifted substantially from their aqueous-solution values.[46] A thermodynamic cycle can be drawn connecting oxidized and reduced proteins in both folded and unfolded configurations (Figure 1).[45,47] If the active-site reduction potentials are different for the folded and unfolded states ($\Delta E_f^\circ \equiv E_F^\circ - E_U^\circ$), then the free energies of folding the oxidized and reduced proteins will differ by a comparable amount ($\Delta\Delta G_f^\circ \equiv \Delta G_{f,OX}^\circ - \Delta G_{f,RED}^\circ$).

Under normal conditions in aqueous solution, both the oxidized and reduced forms of redox proteins are usually folded; ΔE_f° reflects the relative stabilities of the two forms. Addition of denaturants (e.g., urea, guanidine hydrochloride (GuHCl)) to protein solutions induces unfolding; the folding free energies under these conditions (ΔG_f) often are found to be linear functions of the denaturant concentration ([D], eq 1).[48,49] Indeed, linear

$$\Delta G_f = \Delta G_f^\circ + m_D[D] \qquad (1)$$

extrapolation to infinite dilution of a ΔG_f vs [D] plot is commonly employed to estimate ΔG_f°.[50] In redox proteins with large values of ΔE_f°, and comparable values of

Jason R. Telford worked with Ken Raymond at the University of California at Berkeley (Ph.D., 1995); he was a Postdoctoral Scholar at Caltech (1996−98) and is now at the University of Iowa.

Pernilla Wittung-Stafshede worked with Bengt Nordén at Chalmers Institute of Technology in Göteborg, Sweden (Ph.D., 1996); she was a Postdoctoral Scholar at Caltech (1997−98) and is now on the faculty at Tulane University.

Harry B. Gray studied inorganic chemistry at Northwestern University (1957−60) and the University of Copenhagen (1960−61) before joining the chemistry faculty of Columbia University. In 1966, he moved to Caltech, where he is the Arnold O. Beckman Professor of Chemistry and Director of the Beckman Institute.

Jay R. Winkler (Ph.D., 1984, Caltech) is Director of the Laser Resource Center and Member of the Beckman Institute. He moved to Caltech in 1990 from Brookhaven National Laboratory.

10.1021/ar970078t CCC: $15.00
Published on Web 10/28/1998

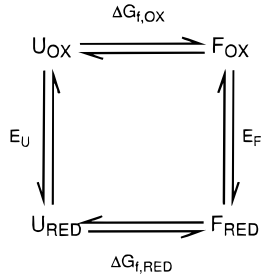

FIGURE 1. Thermodynamic cycle illustrating the relationship between the reduction potentials (E_F, E_U) for folded (F) and unfolded (U) proteins and the folding free energies of oxidized ($\Delta G_{f,OX}$) and reduced proteins ($\Delta G_{f,RED}$).

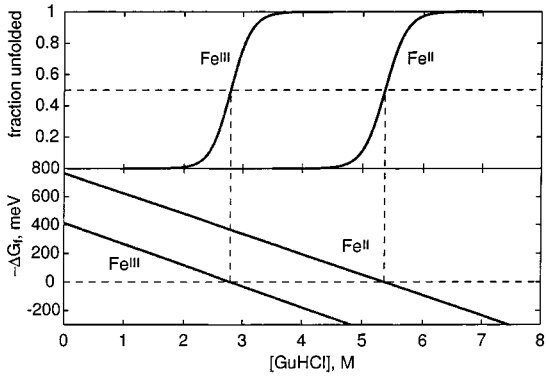

FIGURE 2. (Top) Equilibrium unfolding curves for oxidized (Fe^{III}) and reduced (Fe^{II}) horse heart cytochrome *c*. (Bottom) Folding free energies as functions of denaturant concentration.

$m_{D,OX}$ and $m_{D,RED}$, it is possible to find denaturing conditions where one oxidation state of the protein is fully unfolded while the other is fully folded.[51] The coupling of folding free energies and redox potentials is clearly illustrated by the unfolding behavior of horse heart cytochrome *c* (Figure 2).[45,52,53] In the folded protein, the formal potential of the redox-active (heme) cofactor is 0.38 eV greater than its value in aqueous solution. Consequently, the reduced protein has a more favorable folding free energy than the oxidized protein ($\Delta\Delta G_f^\circ = 42$ kJ mol^{-1}). The unfolding midpoints occur at denaturant concentrations of 2.8 M ($\Delta G_{f,OX}^\circ / m_{D,OX}$) and 5.3 M ($\Delta G_{f,RED}^\circ / m_{D,RED}$) for oxidized and reduced proteins, respectively. Notably, the values of $m_{D,OX}$ and $m_{D,RED}$ are quite similar (14.3 and 13.8 kJ mol^{-1} M^{-1}, respectively).[53] There is a range of denaturant concentrations in which ≥99% of the oxidized protein is unfolded and ≥99% of the reduced protein is folded. In this range, electron injection into the ferriheme of the unfolded protein will initiate a folding reaction. Similarly, electron removal from the reduced folded protein will induce unfolding. Thus far, our investigations of folding kinetics have been restricted to heme proteins in which the driving force for folding is greater in the reduced form.[45,52,54,55]

Photochemical Electron-Transfer Triggers

An attractive feature of ET-triggered folding is the availability of many well-established techniques for rapidly injecting and removing electrons from proteins on time scales as short as a few nanoseconds. Electronically excited $Ru(bpy)_3^{2+}$ ($^*Ru(bpy)_3^{2+}$; bpy = 2,2′-bipyridine) is a powerful reductant ($E^\circ(Ru^{3+/*2+}) = -0.85$ V vs NHE), and its 600-ns decay time makes it an excellent reagent for triggering folding reactions on the microsecond time scale.[45] Furthermore, the millisecond-time-scale reoxidation of the reduced protein by $Ru(bpy)_3^{3+}$ regenerates the initial species and permits extensive signal averaging.

Complete folding of a protein can require tens to hundreds of milliseconds. Consequently, irreversible photochemical ET reagents are required to study the entire range of folding dynamics. Early on, we found that UV irradiation of $Co(ox)_3^{3-}$ (ox = $C_2O_4^{2-}$) produces Co_{aq}^{2+} and a species, presumably $CO_2^{\bullet-}$, that can reduce an unfolded heme protein.[45] Unlike $^*Ru(bpy)_3^{2+}$, $CO_2^{\bullet-}$ does not decay rapidly in solution; the reduction time scale is determined by the pseudo-first-order rate constant for ET to the unfolded heme protein (~1 ms under typical conditions). Under some conditions, however, oxidation of the unfolded reduced protein by $Co(ox)_3^{3-}$ competes with folding.

We have found that NADH is the best irreversible photochemical sensitizer for injecting electrons into unfolded proteins.[54,56] Two-photon, 355-nm excitation of this reagent generates two powerful reductants, a solvated electron and NAD$^\bullet$;[57] both reductants reduce unfolded heme proteins (~100 μM) in about 100 μs. The combination of $^*Ru(bpy)_3^{2+}$ and NADH permits investigations of 1 μs to >1 s folding events of heme proteins.

Cytochrome *c*

The folding of Fe^{III}-cyt *c* (Figure 3) has been studied by several investigators.[12,19,26,28,33,35−37,58−62] The unfolded protein has a low-spin heme with one native axial His ligand (His18) and a nonnative His ligand that replaces the Met80 of the folded structure ($(His)_2Fe^{III}$-cyt_U *c*).[63−66] Recent evidence indicates that His33 is bound to the heme in the unfolded protein above pH 5.5.[65] When the nonnative His ligand is dissociated from the heme by protonation (below pH 5.5), or is removed by site-directed mutagenesis, Fe^{III}-cyt_U *c* folding is accelerated.[12,36,58,65] It appears that substitution of the nonnative His ligand limits the rate of Fe^{III}-cyt_U *c* folding at neutral pH. Thus, the low-spin, bis-His-ligated heme represents a folding trap; correct ligation is required before the protein can fold properly.

The folding of oxidized cytochrome *c* has been examined far more extensively than that of the reduced protein.[11] Given the key role of axial-ligand binding in ferricytochrome *c* folding, and the substantially greater folding stability of ferrocytochrome *c*, it is possible that the mechanism of folding the reduced protein differs significantly from that of the oxidized protein. Our initial investigations of ET-triggered Fe^{II}-cyt_U *c* folding employed $Co(ox)_3^{3-}$ as the sensitizer for electron injection; the studies were perforce limited to folding events on millisecond and longer time scales.[45,52] At neutral pH, the folding of horse heart Fe^{II}-cyt_U *c* is accompanied by a

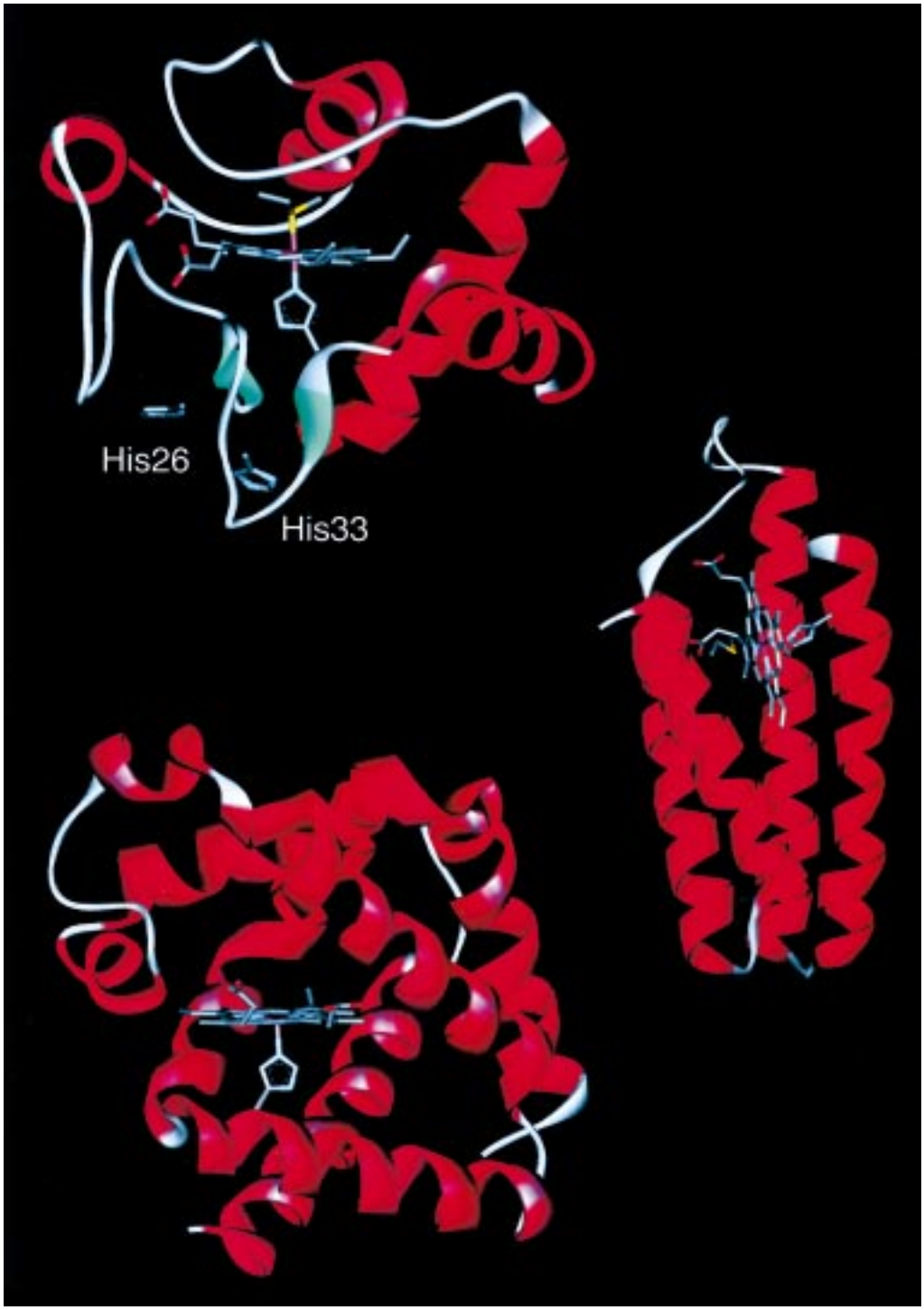

FIGURE 3. Ribbon structures of horse heart cytochrome *c* (top), cytochrome b_{562} (middle), and sperm whale myoglobin (bottom).

significant change in the heme absorption spectrum on a time scale of tens to hundreds of milliseconds. The average rate constant for this phase decreases exponentially with increasing denaturant concentration. This result implies a linear relationship between the activation free energy and the free-energy change for the folding reaction. Similar correlations have been observed in the folding of several other proteins.[21,23,26,48] The folding rates of horse and *Saccharomyces cerevisiae* cytochromes *c* agree well when they are normalized to a constant folding free-energy change (Figure 4).[52] This observation indicates that, although the folding rates vary with GuHCl concentration, they do so because of a shift in the position of the folding/unfolding equilibrium, and not because GuHCl is a specific reactant in the folding process.

The study of ferrocytochrome *c* folding initiated by CO dissociation from (CO)Fe^{II}-cyt_U *c* suggested that Met80 binding, with a time constant of ~40 μs, was the first step in the process.[11,67,68] This result contrasts sharply with ferricytochrome *c* folding, and may be due to the absence of the nonnative His ligand in the initial unfolded state. ET-triggered folding experiments begin with Fe^{III}-cyt_U *c*,

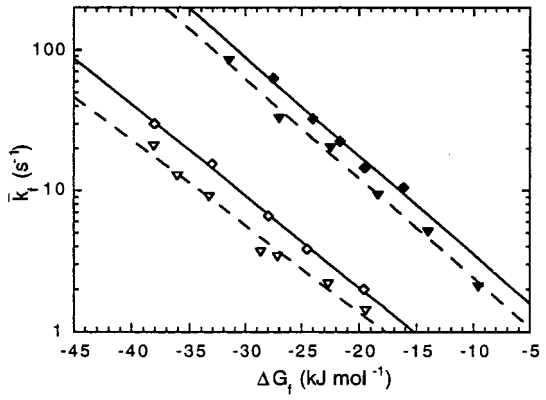

FIGURE 4. Mean cytochrome *c* folding rates as a function of driving force: horse heart cytochrome *c* (22.5 °C, ◇; 40.0 °C, ◆); yeast cytochrome *c* (22.5 °C, ▽; 40.0 °C, ▼).

which is likely to have a structure substantially different from that of (CO)Fe^{II}-cyt_U *c*.[69] At the very least, the initial ligation state of the heme when folding is initiated by CO dissociation will not be the same as that in ET-triggered folding. For this reason, the sequence of steps in the folding of these two structures could differ substantially.

To test the role of histidine residues in ferrocytochrome *c* folding, we have examined the dynamics of folding and the concurrent spectral changes of Fe^{II}-cyt *c* between 10 μs and 1 s, over a range of pH and as a function of added ligands.[56] We use *N*-acetylmicroperoxidase-8 (MP8), the heme octapeptide produced by enzymatic digestion of cytochrome *c*,[70] as a spectroscopic model complex for the unfolded protein. This water-soluble heme peptide, containing residues 14−21 from the original protein, retains the His18 axial heme ligand, as well as the key thioether links between the porphyrin and Cys residues at positions 14 and 17. The spectra and kinetics obtained following electron injection into Fe^{III}-MP8 serve as a guide to the interpretation of the results with cytochrome *c*.

The early events in Fe^{II}-cyt_U *c* folding have been examined using *$Ru(bpy)_3^{2+}$ as the photochemical sensitizer.[45,56] In 3.5 M GuHCl, the first-order decay rate for *$Ru(bpy)_3^{2+}$ is a linear function of the concentration of Fe^{III}-cyt_U *c*. This observation is consistent with a bimolecular ET reaction between *$Ru(bpy)_3^{2+}$ and Fe^{III}-cyt_U *c*. Following the initial phase of protein reduction, a second process with a time constant of ~20 μs can be detected by transient absorption spectroscopy. The rate constant for this phase varies linearly with protein concentration with an intercept of $\sim 1 \times 10^4$ s^{-1}. Similar results are obtained when the unfolded protein is replaced with MP8 and imidazole−MP8. The time scale of this process is close to that reported for Met80 binding,[11,68] but in ET-triggered folding this phase does not arise from coordination of Met80 to the ferroheme.

After the rapid change in absorbance following electron injection into unfolded cytochrome *c*, there is no substantial variation in the spectrum of the reduced protein for a time period up to 200 μs. Consequently, we used NADH as the sensitizer to study ferrocytochrome *c* folding between 100 μs and 1 s. Following reduction of horse heart Fe^{II}-cyt_U *c* at pH 7 ([GuHCl] = 3.2 M), the transient

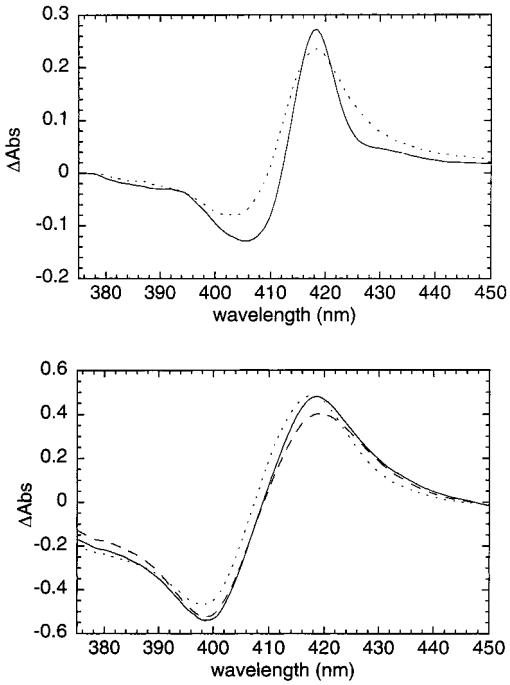

FIGURE 5. Time-resolved difference spectra of horse heart cytochrome *c* following photochemical reduction of the unfolded protein with NADH: (a, top) pH 7, [GuHCl] = 3.2 M, 1 ms (solid line) and 400 ms (dotted line) after excitation; (b, bottom) pH 5, [GuHCl] = 3.1 M, 100 μs (solid line), 1 ms (dashed line), and 400 ms (dotted line) after excitation.

difference spectrum is characteristic of a low-spin, six-coordinate ferroheme (Figure 5a), suggesting that the ferrous ion in the unfolded protein remains axially coordinated to two His ligands. Only minor changes in Soret absorbance are observed in the time range from a few microseconds to several milliseconds after electron injection; significant changes in the heme spectrum occur 50−100 ms after injection. The difference spectrum measured 400 ms after reduction of Fe^{II}-cyt_U *c* closely matches that of folded Fe^{II}-cyt *c* (Figure 5a). Importantly, we see no evidence for a high-spin intermediate in the folding of Fe^{II}-cyt *c* at neutral pH.

The heme axial-ligand set in unfolded cytochrome *c* is a sensitive function of the solution pH. At lower pH, nonnative histidine binding is disfavored ($pK_a \approx 5.3$); the oxidized heme is high-spin, and the axial ligands are His18 and water ($(H_2O)(His)Fe^{III}$-cyt_U *c*).[56,63−65] Under such conditions, Fe^{III}-cyt_U *c* folding is markedly faster than at neutral pH, and a single kinetics phase is observed when folding is probed by Trp fluorescence and S(Met80) → Fe^{III} charge-transfer absorption.[12,13]

We find distinct changes in the folding kinetics of Fe^{II}-cyt_U *c* as the solution pH is lowered.[56] In the unfolded oxidized protein, the acid dissociation constants of the native His18 ligand ($pK_a \approx 2.8$) and the nonnative His ligands are sufficiently close that it is not possible to work at a pH where the nonnative His ligands are fully dissociated, yet the native His18 remains bound. Accordingly, we have examined the ET-triggered folding kinetics of ferrocytochrome *c* near pH 5 where 67% of the unfolded ferric protein is in the high-spin aquo form ((H_2O)(His)-

Fe^{III}-cyt_U *c*) and 33% remains as a low-spin bis-His species ($(His)_2Fe^{III}$-cyt_U *c*). The reduction potential of imidazole−MP8 is shifted ~40 mV negative from that of aquo MP8,[71] indicating that the binding constant for the second imidazole group is smaller for the ferroheme than for the ferriheme, consistent with $pK_a \approx 5.5$ for the nonnative His ligand in the reduced unfolded protein.[56] Hence, at pH 5, only 24% of the unfolded reduced protein should have bis-His ligation ($(His)_2Fe^{II}$-cyt_U *c*). The majority fraction of the reduced unfolded protein at pH 5 is high-spin and, by analogy to deoxymyoglobin,[72] probably five-coordinate ($(His)Fe^{II}$-cyt_U *c*).

As we drop the pH below 7, the observed rates of ferrocytochrome *c* folding increase slightly but remain monoexponential down to pH ≈ 5.5. Below pH 5.5, however, the folding kinetics are distinctly biphasic. The rate constant for the faster process is sensitive to pH, increasing by an order of magnitude between pH 5.5 and pH 4.9. The spectroscopic changes that accompany this phase are consistent with a loss of the nonnative His ligand and conversion from $(His)_2Fe^{II}$-cyt_U *c* to $(His)Fe^{II}$-cyt_U *c* (Figure 5b). The rate of the slower phase does not vary substantially with pH, remaining constant within error at $k_{obs} = 16(5)\ s^{-1}$. The changes in absorption spectra associated with the slow phase are consistent with conversion of $(His)Fe^{II}$-cyt_U *c* to the native, six-coordinate, low-spin His-Met-heme ($(His)(Met)Fe^{II}$-cyt *c*). Thus, the rate of intramolecular methionine ligation to the ferroheme in ET-triggered folding is 16(5) s^{-1} at pH 5, [GuHCl] = 3.1 M. The rate of this step is much slower than the rate reported for Met binding ($2.5 \times 10^4\ s^{-1}$) when folding is initiated by CO dissociation from unfolded carbonmonoxy ferrocytochrome *c*.[11,67,68]

Our transient absorption measurements of ET-triggered ferrocytochrome *c* folding reveal a central role for ligand binding and dissociation kinetics. This is due in large part to the fact that the heme spectrum is far more sensitive to the Fe coordination sphere than it is to the polypeptide conformation. A three-component kinetics model describes our observations:

$$(His)_2Fe^{II}\text{-cyt } c \underset{k_{+His}}{\overset{k_{-His}}{\rightleftharpoons}} (His)Fe^{II}\text{-cyt } c \xrightarrow{k_{+Met}} (His)(Met)Fe^{II}\text{-cyt } c$$

The general solution to the rate law for this model predicts biphasic kinetics. Above pH 6, ferrocytochrome *c* folding is slow and monophasic ($k_{obs} = 1-20\ s^{-1}$; [GuHCl] = 3.1 M). Since we observe only $(His)_2Fe^{II}$-cyt *c* and $(His)(Met)Fe^{II}$-cyt *c*, we can invoke the steady-state approximation for $(His)Fe^{II}$-cyt *c*. In this limit, the kinetics will be exponential with an observed rate constant given by

$$k_{obsd} = \frac{k_{-His}\, k_{+Met}}{k_{+His} + k_{+Met}}$$

At high pH, then, folding could be limited by Met80 binding ($k_{+His} \gg k_{+Met}$; $k_{obsd} \approx k_{+Met}k_{-His}/k_{+His}$) or by nonnative His dissociation ($k_{+Met} \gg k_{+His}$; $k_{obsd} \approx k_{-His}$).

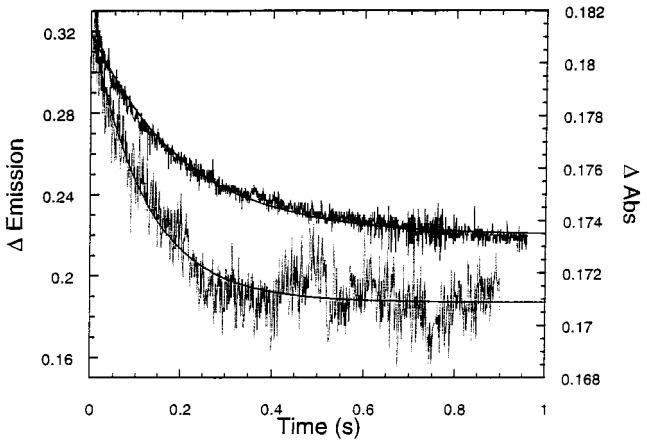

FIGURE 6. Folding kinetics of dansylated yeast ferrocytocytochrome *c* as probed by heme absorption (black) and dansyl fluorescence (gray) (pH 7, [GuHCl] = 1.8 M).

Below pH 6, the folding kinetics are biphasic, and all three of the ligation states of the reduced heme can be detected in the transient absorption spectra. Under these conditions, the steady-state approximation is not valid. The faster kinetics phase reflects the equilibration between $(His)_2Fe^{II}$-cyt *c* and $(His)Fe^{II}$-cyt *c*, with a pH-dependent rate constant given by $k_{+His} + k_{-His}$. The rate constant for the slower step corresponds to $k_{+Met} = 16(5)\ s^{-1}$. If k_{+Met} does not vary substantially with pH, then it is likely that k_{-His} limits ferrocytochrome *c* folding above pH 6.

We have recently studied the folding of reduced *S. cerevisiae* cytochrome *c* with a probe (a dansyl fluorophore) at Cys102.[73] In the folded protein, the dansyl fluorescence is strongly quenched, presumably via energy transfer to the heme. Unfolding the protein with GuHCl restores the dansyl fluorescence. The GuHCl-induced unfolding monitored by dansyl fluorescence matches that monitored by changes in heme absorption, and the presence of the dansyl group only slightly destabilizes the folded protein. The intensity of fluorescence from this dansyl probe located on the C-terminal helix of the folded protein reports on its proximity to the heme. Following photochemical electron injection into Fe^{III}-cyt_U *c* with NADH (pH 7, [GuHCl] ≈ 3.1 M), we observe a rapid decrease in the intensity of the dansyl fluorescence. The time constant for this process (~100 μs) is similar to that for electron injection into Fe^{III}-cyt_U *c*. This phase, which accounts for ~25% of the total reduction in dansyl fluorescence upon folding, also is observed at higher GuHCl concetrations (6 M) where Fe^{III}-cyt_U *c* does not fold. This step is followed by a further decrease in fluorescence on the 10−100-ms time scale. Interestingly, the rate constant for this phase is about a factor of 2 larger than that obtained from changes in heme absorption under identical conditions (Figure 6). These data suggest that the large-scale motions required to position the C-terminal helix occur before the heme−ligand exchange step that limits formation of folded ferrocytochrome *c* at pH 7. This observation is consistent with studies that suggest the C- and N-terminal helices are among the most

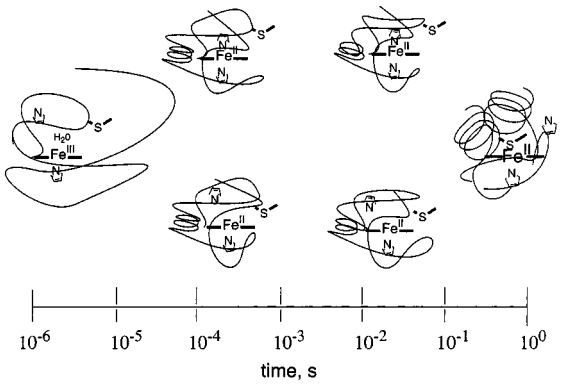

FIGURE 7. Schematic representation of ferrocytochrome *c* folding at high (upper path) and low (lower path) pH. Reduction of unfolded ferricytochrome *c* is complete within 100 μs. The protein subsequently collapses and develops secondary structure, but Met80 binding to form the native structure requires more than 100 ms to complete.

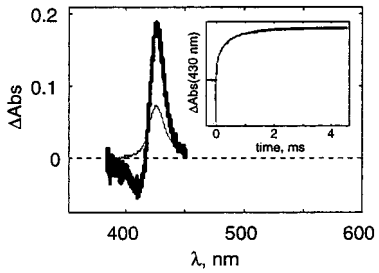

FIGURE 8. Transient absorption kinetics (430 nm, inset) and spectra recorded 200 μs (thin line) and 2 ms (thick line) after electron injection into unfolded ferricytochrome b_{562} (pH 7, [GuHCl] = 2.25 M).

stable and earliest formed structural domains in folded ferricytochrome *c*.[26,60]

Our time-resolved absorption and luminescence measurements permit us to develop a rudimentary picture of ferrocytochrome *c* folding (Figure 7). The 10−100-ms decrease in dansyl fluorescence following reduction of Fe^{III}-cyt_U *c* suggests a collapse of the protein to a more compact form. The final step in the folding process coincides with Met80 ligation, a process that appears to be limited by dissociation of nonnative His ligands above pH 7. Although ligand substitution is central to the formation of the native folded structure of ferrocytochrome *c*, these steps must be coupled to rearrangements of the polypeptide. The finding that folding rates measured by transient absorption at pH 7 correlate well with folding free-energy changes,[45] and that cytochromes *c* from different species fold at comparable rates when the folding driving forces are matched,[52] indicates that k_{+His}, k_{-His}, and k_{+Met} are closely tied to the folding of the polypeptide.

Cytochrome b_{562}

A requirement for kinetics studies of folding is that the redox-active cofactor remain bound to the unfolded protein. When the cofactor is dissociated from the unfolded protein, its bimolecular capture would likely be the rate-limiting process. Originally, we believed that this requirement would limit our investigations to proteins with covalently bound redox-active cofactors. We have demonstrated, however, that ET triggering can be employed to study the folding of a four-helix-bundle protein, cytochrome b_{562}.[54] Although the porphyrin is not covalently attached to the protein, the heme iron is ligated axially by the side chains of Met7 and His102 (Figure 3).

As expected for a heme protein with a 0.18-V reduction potential, titrations with GuHCl confirm that reduced cytochrome b_{562} is more stable toward unfolding than the oxidized protein.[54,74,75] Unfolding experiments probed using circular dichroism and Soret-band absorbance gave identical results, consistent with a two-state process. In contrast to the bis-His ligation of unfolded cytochrome *c*, absorption spectra of the unfolded cytochrome b_{562} indicate that the heme iron is high-spin in both oxidation states. Oxidized cytochrome b_{562} is fully denatured at 2 M GuHCl, whereas reduced cytochrome b_{562} does not unfold below 6 M GuHCl. The oxidized protein refolds upon dilution of GuHCl, and the refolding kinetics show no protein-concentration dependence, indicating that the heme is still associated with the protein in the unfolded state. It is likely that the Fe^{III}−N(His102) bond is still intact in the unfolded protein.

Electron injection into unfolded, oxidized cytochrome b_{562} (Fe^{III}-cyt_U b_{562}) produces a significant amount of folded, reduced protein (Fe^{II}-cyt_F b_{562}) at GuHCl concentrations between 2 and 3 M. The transient difference spectrum measured 200 μs after laser excitation of NADH in the presence of Fe^{III}-cyt_U b_{562} (Figure 8) is consistent with that of a high-spin Fe^{II} heme. The spectrum measured 2 ms after excitation (Figure 8) indicates the formation of a low-spin Fe^{II} heme, and closely matches that expected for Fe^{II}-cyt_F b_{562}. The ferrocytochrome b_{562} folding kinetics can be described by a dominant kinetic phase with a first-order rate constant of 800 ± 200 s^{-1} at a driving force of ~25 kJ/mol (2.5 M GuHCl). At a similar driving force, Fe^{II}-cyt_U *c* folds much more slowly (10 s^{-1}). The absence of nonnative His ligands is certainly one explanation for the faster folding of cytochrome b_{562}, but even at reduced pH, the rate of Met80 binding to the ferroheme in cytochrome *c* (16(5) s^{-1}) is far slower than in cytochrome b_{562}.

Myoglobin

Sperm whale myoglobin (Mb) is another heme protein with a noncovalently attached porphyrin (Figure 3).[72] The heme in Mb is coordinated to a single axial histidine ligand, and both oxidized (ferric or met) and reduced (ferrous or deoxy) states have a high-spin electronic configuration. As was found for both cytochrome *c* and cytochrome b_{562}, the reduced form of the protein is more stable than the oxidized form.[55] Between 2.5 and 3 M GuHCl, where Fe^{III}-Mb is fully unfolded, addition of dithionite leads to the formation of folded Fe^{II}-Mb. We found only a 20−25% yield of folded Fe^{II}-Mb in these experiments, presumably because heme dissociation competes with the folding of the reduced protein.

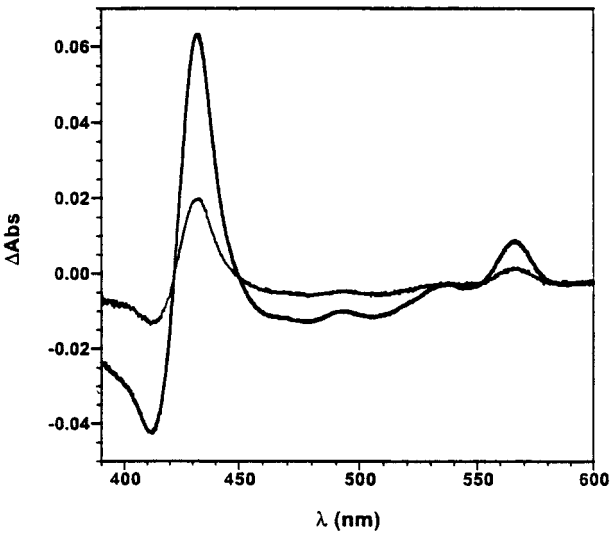

FIGURE 9. Transient absorption spectra recorded 100 μs (thin line) and 10 ms (thick line) after electron injection into unfolded sperm whale myoglobin.

Laser excitation of NADH generates species that reduce Fe^{III}-Mb; the pseudo-first-order rate constant for this reduction was found to be 2.4(6) $\times$ 10^4 s^{-1} (100 μM protein). Reduction of unfolded Fe^{III}-Mb to unfolded Fe^{II}-Mb does not result in large absorption changes, whereas the difference spectrum associated with the conversion of unfolded to folded Fe^{II}-Mb is quite distinctive. The difference spectrum obtained from measurements on samples before and after 355-nm excitation of NADH agrees with the calculated difference spectrum between unfolded Fe^{III}-Mb and folded Fe^{II}-Mb, confirming that folding occurs. Moreover, the difference spectrum recorded 10 ms after excitation demonstrates the formation of folded Fe^{II}-Mb (Figure 9). The kinetics of Fe^{II}-Mb folding at a driving force of ~10 kJ/mol (2.5 M GuHCl) are independent of protein concentration; the rate constant is 5(2) $\times$ 10^3 s^{-1}.

Summary and Prospects

Cytochrome *c* folds at least 50 times slower than myoglobin or cytochrome b_{562}. In cytochrome b_{562} the tertiary fold can be approximated as a symmetric bundle of four cylinders. Upon reduction of the heme, the α-helices cluster around the heme, and the methionine sulfur bonds to iron, yielding the final low-spin complex. It is of interest to note that the folding of a four-helix bundle without a cofactor, acyl coenzyme A binding protein, proceeds on a time scale comparable to that of Fe^{II}-cyt_U b_{562} (<5 ms at room temperature[23]), and deoxymyoglobin folds even faster. In accord with theoretical analyses, then, it would appear that highly helical proteins have favorable energy landscapes for folding.[76]

Oxidation-state-dependent folding free energies are a general property of redox-active proteins. ET-triggering has allowed us to examine the folding of proteins that would be difficult or impossible to study by other methods, and with time resolution great enough to permit investigations of the earliest steps of the folding process. The folding of many more proteins could be triggered by this technique because redox cofactors tend to remain bound to unfolded proteins. The challenge now is to exploit existing probes and develop new probes that report on the structure of a protein as it folds. Absorption spectroscopy has revealed details of the metal−ligand environment during folding of polypeptides around hemes, and this method promises to provide information about the development of blue and purple centers that must accompany the formation of folded copper proteins.[51] Fluorescent probes bound to specific sites in proteins are sensitive to structures at long distances from the redox cofactor, and vibrational spectroscopy (infrared and Raman) can be employed to study the development of secondary structure. The combination of new triggers and new folding probes promises to provide increasingly detailed information about how unfolded proteins find their way to unique, stable structures.

This work was supported by the NSF (Grant MCB-9630465 to J.R.W.; Grant CHE-9508533 to H.B.G.). Postdoctoral fellowships from the NIH (J.R.T.) and TFR-Sweden (P.W.-S.) are acknowledged with thanks. Important contributions to our ET-triggered folding studies have been made by Gary Mines, John Chesick, Sonny Lee, Don Low, Bo Malmström, Torbjörn Pascher, and F. Akif Tezcan. We also thank Bill Eaton, George McLendon, José Onuchic, and Peter Wolynes for helpful discussions. H.B.G. thanks Balliol College and the Inorganic Chemistry Laboratory, University of Oxford, for providing a stimulating intellectual environment during 1997−98.

References

(1) Bryngelson, J. D.; Onuchic, J. N.; Wolynes, P. G. Funnels, Pathways and the Energy Landscape of Protein Folding − A Synthesis. *Proteins: Struct., Funct., Genet.* **1995**, *21*, 167−195.
(2) Dill, K. A.; Chan, H. S. From Levinthal to Pathways to Funnels. *Nat. Struct. Biol.* **1997**, *4*, 10−19.
(3) Shakhnovich, E. I. Theoretical Studies of Protein-Folding Thermodynamics and Kinetics. *Curr. Opin. Struct. Biol.* **1997**, *7*, 29−40.
(4) Lazaridis, T.; Karplus, M. "New View" of Protein Folding Reconciled with the Old Through Multiple Unfolding Simulations. *Science* **1997**, *278*, 1928−1931.
(5) Onuchic, J. N.; Lutheyschulten, Z.; Wolynes, P. G. Theory of Protein-Folding − the Energy Landscape Perspective. *Annu. Rev. Phys. Chem.* **1997**, *48*, 545−600.
(6) Chen, L. X.-Q.; Petrich, J. W.; Fleming, G. R.; Perico, A. Picosecond Fluorescence Studies of Polypeptide Dynamics: Fluorescence Anisotropies and Lifetimes. *Chem. Phys. Lett.* **1987**, *139*, 55−61.
(7) Williams, S.; Causgrove, T. P.; Gilmanshin, R.; Fang, K. S.; Callender, R. H.; Woodruff, W. H.; Dyer, R. B. Fast Events in Protein Folding: Helix Melting and Formation in a Small Peptide. *Biochemistry* **1996**, *35*, 691−697.
(8) Koide, S.; Dyson, H. J.; Wright, P. E. Characterization of a Folding Intermediate of Apoplastocyanin Trapped by Proline Isomerization. *Biochemistry* **1993**, *32*, 12299−12310.
(9) Karplus, M.; Weaver, D. L. Protein Folding Dynamics: The Diffusion-Collision Model and Experimental Data. *Protein Sci.* **1994**, *3*, 650−668.

(10) Zwanzig, R. Simple Model of Protein Folding Kinetics. *Proc. Natl. Acad. Sci. U.S.A.* **1995**, *92*, 9801−9804.
(11) Jones, C. M.; Henry, E. R.; Hu, Y.; Chan, C.-K.; Luck, S. D.; Bhuyan, A.; Roder, H.; Hofrichter, J.; Eaton, W. A. Fast Events in Protein Folding Initiated by Nanosecond Laser Photolysis. *Proc. Natl. Acad. Sci. U.S.A.* **1993**, *90*, 11860−11864.
(12) Elöve, G.; Bhuyan, A. K.; Roder, H. Kinetic Mechanism of Cytochrome *c* Folding: Involvement of the Heme and its Ligands. *Biochemistry* **1994**, *33*, 6925−6935.
(13) Sosnick, T. R.; Mayne, L.; Hiller, R.; Englander, S. W. The Barriers in Protein Folding. *Nat. Struct. Biol.* **1994**, *1*, 149−156.
(14) Baldwin, R. L. Finding Intermediates in Protein Folding. *BioEssays* **1994**, *16*, 207−210.
(15) Fersht, A. R. Characterizing Transition States in Protein Folding: an Essential Step in the Puzzle. *Curr. Opin. Struct. Biol.* **1995**, *5*, 79−84.
(16) Ptitsyn, O. B. Molten Globule and Protein Folding. *Adv. Protein Chem.* **1995**, *47*, 83−229.
(17) Englander, S. W.; Mayne, L. Protein Folding Studies Using Hydrogen-Exchange Labeling and Two-Dimensional NMR. *Annu. Rev. Biophys. Biomol. Struct.* **1992**, *21*, 243−265.
(18) Plaxco, K.; Dobson, C. M. Time-Resolved Biophysical Methods in the Study of Protein Folding. *Curr. Opin. Struct. Biol.* **1996**, *6*, 630−636.
(19) Kuwajima, K.; Yamaya, H.; Miwa, S.; Sugai, S.; Nagamura, T. Rapid Formation of Secondary Structure Framework in Protein Folding Studied by Stopped-Flow Circular Dichroism. *FEBS Lett.* **1987**, *221*, 115−118.
(20) Milla, M. E.; Brown, B. M.; Waldburger, C. D.; Sauer, R. T. P22 Arc Repressor: Transition State Properties Inferred from Mutational Effects on the Rates of Protein Unfolding and Refolding. *Biochemistry* **1995**, *34*, 13914−13919.
(21) Villegas, V.; Azuaga, A.; Catasús, L.; Reverter, D.; Mateo, P. L.; Avilés, F. X.; Serrano, L. Evidence for a Two-State Transition in the Folding Process of the Activation Domain of Human Procarboxypeptidase A2. *Biochemistry* **1995**, *34*, 15105−15110.
(22) Hooke, S. D.; Radford, S. E.; Dobson, C. M. The Refolding of Human Lysozyme: A Comparison with the Structurally Homologous Hen Lysozyme. *Biochemistry* **1994**, *33*, 5867−5876.
(23) Kragelund, B. B.; Robinson, C. V.; Knudsen, J.; Dobson, C. M.; Poulsen, F. M. Folding of a Four-Helix Bundle: Studies of Acyl-Coenzyme A Binding Protein. *Biochemistry* **1995**, *34*, 7217−7224.
(24) Woodward, C. K. Hydrogen Exchange Rates and Protein Folding. *Curr. Opin. Struct. Biol.* **1994**, *4*, 112−116.
(25) Plaxco, K. W.; Claus, S.; Campbell, I. D.; Dobson, C. M. Rapid Refolding of a Proline-Rich All-Beta-Sheet Fibronectin Type III Module. *Proc. Natl. Acad. Sci. U.S.A.* **1996**, *93*, 10703−10706.
(26) Bai, Y.; Sosnick, T. R.; Mayne, L.; Englander, S. W. Protein Folding Intermediates: Native-State Hydrogen Exchange. *Science* **1995**, *269*, 192−197.
(27) Englander, S. W.; Mayne, L.; Bai, Y.; Sosnick, T. R. Hydrogen Exchange: The Modern Legacy of Linderstrøm-Lang. *Protein Sci.* **1997**, *6*, 1101−1109.
(28) Elöve, G. A.; Chaffotte, A. F.; Roder, H.; Goldberg, M. Early Steps in Cytochrome *c* Folding Probed by Time-Resolved Circular Dichroism and Fluorescence Spectroscopy. *Biochemistry* **1992**, *31*, 6876−6883.
(29) Houry, W. A.; Rothwarf, D. M.; Scheraga, H. A. Circular Dichroism Evidence for the Presence of Burst-Phase Intermediates on the Conformational Folding Pathway of Ribonuclease A. *Biochemistry* **1996**, *35*, 10125−10133.
(30) Arai, M.; Kuwajima, K. Rapid Formation of a Molten Globule Intermediate in Refolding of α-Lactalbumin. *Folding Des.* **1996**, *1*, 275−287.
(31) Yamasaki, K.; Ogasahara, K.; Yutani, K.; Oobatake, M.; Kanaya, S. Folding Pathway of *Escherichia coli* Ribonuclease HI: A Circular Dichroism, Fluorescence, and NMR Study. *Biochemistry* **1995**, *34*, 16552−16562.
(32) Jones, B. E.; Beechem, J. M.; Matthews, C. R. Local and Global Dynamics during the Folding of *Escherichia coli* Dihydrofolate Reductase by Time-Resolved Fluorescence Spectroscopy. *Biochemistry* **1995**, *34*, 1867−1877.
(33) Chan, C. K.; Hu, Y.; Takahashi, S.; Rousseau, D. L.; Eaton, W. A.; Hofrichter, J. Submillisecond Protein-Folding Kinetics Studied by Ultrarapid Mixing. *Proc. Natl. Acad. Sci. U.S.A.* **1997**, *94*, 1779−1784.
(34) Chan, C. K.; Eaton, W. A.; Hofrichter, J. Submillisecond Processes in Protein Folding Studied by Ultrarapid Mixing and Continuous Flow. *Biophys. J.* **1997**, *72*, 383.
(35) Takahashi, S.; Yeh, S.-R.; Das, T. K.; Chan, C.-K.; Gottfried, D. S.; Rousseau, D. L. Folding of Cytochrome *c* Initiated by Submillisecond Mixing. *Nat. Struct. Biol.* **1997**, *4*, 44−50.
(36) Yeh, S.-R.; Takahashi, S.; Fan, B.; Rousseau, D. L. Ligand Exchange During Cytochrome *c* Folding. *Nat. Struct. Biol.* **1997**, *4*, 51−56.
(37) Shastry, M. C. R.; Roder, H. Evidence for Barrier-Limited Protein-Folding Kinetics on the Microsecond Time-Scale. *Nat. Struct. Biol.* **1998**, *5*, 385−392.
(38) Nölting, B.; Golbik, R.; Fersht, A. R. Submillisecond Events in Protein Folding. *Proc. Natl. Acad. Sci. U.S.A.* **1995**, *92*, 10668−10672.
(39) Nölting, B.; Golbik, R.; Niera, J. L.; Soler-Gonzalez, A. S.; Schreiber, G.; Fersht, A. R. The Folding Pathway of a Protein at High Resolution from Microseconds to Seconds. *Proc. Natl. Acad. Sci. U.S.A.* **1997**, *94*, 826−830.
(40) Ballew, R. M.; Sabelko, J.; Gruebele, M. Direct Observation of Fast Protein Folding: The Initial Collapse of Apomyoglobin. *Proc. Natl. Acad. Sci. U.S.A.* **1996**, *93*, 5759−5764.
(41) Woodruff, W. H.; Dyer, R. B.; Callender, R. H.; Paige, K.; Causgrove, T. Fast Events in Protein Folding − Laser T-jump Time-Resolved Infrared Study of the Ribonuclease-A S-peptide. *Biophys. J.* **1994**, *66*, A397.
(42) Phillips, C. M.; Mizutani, Y.; Hochstrasser, R. M. Ultrafast Thermally Induced Unfolding of RNase A. *Proc. Natl. Acad. Sci. U.S.A.* **1995**, *92*, 7292−7296.
(43) Munoz, V.; Thompson, P. A.; Hofrichter, J.; Eaton, W. A. Folding Dynamics and Mechanism of Beta-Hairpin Formation. *Nature* **1997**, *390*, 196−199.
(44) Thompson, P. A.; Eaton, W. A.; Hofrichter, J. Laser Temperature-Jump Study of the Helix ⇌ Coil Kinetics of an Alanine Peptide Interpreted with a Kinetic Zipper Model. *Biochemistry* **1997**, *36*, 9200−9210.
(45) Pascher, T.; Chesick, J. P.; Winkler, J. R.; Gray, H. B. Protein Folding Triggered by Electron Transfer. *Science* **1996**, *271*, 1558−1560.
(46) Churg, A. K.; Warshel, A. Control of the Redox Potential of Cytochrome *c* and Microscopic Dielectric Effects in Proteins. *Biochemistry* **1986**, *25*, 1675−1681.

(47) Bixler, J.; Bakker, G.; McLendon, G. Electrochemical Probes of Protein Folding. *J. Am. Chem. Soc.* **1992**, *114*, 6938−6939.
(48) Chen, B.-L.; Baase, W. A.; Nicholson, H.; Schellman, J. A. Folding Kinetics of T4 Lysozyme and Nine Mutants at 12 °C *Biochemistry* **1992**, *31*, 1464−1476.
(49) Matouschek, A.; Otzen, D. E.; Itzhaki, L. S.; Jackson, S. E.; Fersht, A. R. Movement of the Position of the Transition State in Protein Folding. *Biochemistry* **1995**, *34*, 13656−13662.
(50) Yao, M.; Bolen, D. W. How Valid are Denaturant-Induced Free Energy Measurements? Level of Confidence to Common Assumptions over an Extended Range of Ribonuclease A Stability. *Biochemistry* **1995**, *34*, 3771−3781.
(51) Winkler, J. R.; Wittung-Stafshede, P.; Leckner, J.; Malmström, B. G.; Gray, H. B. Effects Of Folding On Metalloprotein Active-Sites. *Proc. Natl. Acad. Sci. U.S.A.* **1997**, *94*, 4246−4249.
(52) Mines, G. A.; Pascher, T.; Lee, S. C.; Winkler, J. R.; Gray, H. B. Cytochrome *c* Folding Triggered by Electron Transfer. *Chem. Biol.* **1996**, *3*, 491−497.
(53) Mines, G. A.; Winkler, J. R.; Gray, H. B. Spectroscopic Studies of Ferrocytochrome *c* Folding. In *Spectroscopic Methods in Bioinorganic Chemistry*; Solomon, E. I., Hodgson, K. O., Eds.; American Chemical Society: Washington, DC, 1998.
(54) Wittung-Stafshede, P.; Gray, H. B.; Winkler, J. R. Rapid Formation of a Four Helix Bundle. Cytochrome b_{562} Folding Triggered by Electron Transfer. *J. Am. Chem. Soc.* **1997**, *119*, 9562−9563.
(55) Wittung-Stafshede, P.; Malmström, B. G.; Winkler, J. R.; Gray, H. B. Folding of Deoxymyoglobin Triggered by Electron Transfer. *J. Phys. Chem. A* **1998**, *102*, 5599−5601.
(56) Telford, J. R.; Tezcan, F. A.; Gray, H. B.; Winkler, J. R. Role of Ligand Substitution in Ferrocytochrome *c* Folding. *Biochemistry*, submitted for publication.
(57) Orii, Y. Immediate Reduction of Cytochrome *c* by Photoexcited NADH. Reaction Mechanism as Revealed by Flow Flash and Rapid-Scan Studies. *Biochemistry* **1993**, *32*, 11910−11914.
(58) Sosnick, T. R.; Mayne, L.; Englander, S. W. Molecular Collapse: The Rate-Limiting Step in Two-State Cytochrome *c* Folding. *Proteins: Struct., Funct., Genet.* **1996**, *24*, 413−426.
(59) Sosnick, T. R.; Shtilerman, M. D.; Mayne, L.; Englander, S. W. Ultrafast Signals in Protein Folding and the Polypeptide Contracted State. *Proc. Natl. Acad. Sci. U.S.A.* **1997**, *94*, 8845−8550.
(60) Colón, W.; Elöve, G. A.; Wakem, L. P.; Sherman, F.; Roder, H. Side Chain Packing of the N- and C−Terminal Helices Plays a Critical Role in the Kinetics of Cytochrome *c* Folding. *Biochemistry* **1996**, *35*, 5538−5549.
(61) Pierce, M. M.; Nall, B. T. Fast Folding of Cytochrome *c*. *Protein Sci.* **1997**, *6*, 618−627.
(62) Konermann, L.; Collings, B. A.; Douglas, D. J. Cytochrome *c* Folding Kinetics Studied by Time-Resolved Electrospray Ionization Mass Spectrometry. *Biochemistry* **1997**, *36*, 5554−5559.
(63) Babul, J.; Stellwagen, E. Participation of the Protein Ligands in the Folding of Cytochrome *c*. *Biochemistry* **1972**, *11*, 1195−1200.
(64) Muthukrishnan, K.; Nall, B. T. Effective Concentrations of Amino Acid Side Chains in an Unfolded Protein. *Biochemistry* **1991**, *30*, 4706−4710.
(65) Colón, W.; Wakem, L. P.; Sherman, F.; Roder, H. Identification of the Predominant Non-Native Histidine Ligand in Unfolded Cytochrome *c*. *Biochemistry* **1997**, *36*, 12535−12541.
(66) Godbole, S.; Bowler, B. E. A Histidine Variant of Yeast Iso-1-Cytochrome *c* that Strongly Affects the Energetics of the Denatured State. *J. Mol. Biol.* **1997**, *268*, 816−821.
(67) Chan, C. K.; Hofrichter, J.; Eaton, W. A. Optical Triggers of Protein Folding. *Science* **1996**, *274*, 628−629.
(68) Hagen, S. J.; Hofrichter, J.; Eaton, W. A. Rate of Intrachain Diffusion of Unfolded Cytochrome *c*. *J. Phys. Chem. B* **1997**, *101*, 2352−2365.
(69) Winkler, J. R.; Gray, H. B. Optical Triggers Of Protein Folding − Response. *Science* **1996**, *274*, 629.
(70) Wang, J.-S.; Baek, H. K.; Van Wart, H. E. High-Valent Intermediates in the Reaction of N_α-Acetyl Microperoxidase-8 with Hydrogen Peroxide: Models for Compounds 0, I and II of Horseradish Peroxidase. *Biochem. Biophys. Res. Commun.* **1991**, *179*, 1320−1324.
(71) Tezcan, F. A.; Winkler, J. R.; Gray, H. B. Effects of Ligation and Folding on Reduction Potentials of Heme Proteins. *J. Am. Chem. Soc.*, submitted for publication.
(72) Antonini, E.; Brunori, M. *Hemoglobin and Myoglobin in their Reactions with Ligands*; North-Holland Publishing Co.: Amsterdam, 1971.
(73) Telford, J. R.; Gray, H. B.; Winkler, J. R. To be submitted for publication.
(74) Kita, K.; Konishi, K.; Anraku, Y. Terminal Oxidases of *Escherichia coli* Aerobic Respiratory Chain. 1. Purification and Properties of Cytochrome b_{562}, Complex from Cells in the Early Exponential Phase of Aerobic Growth. *J. Biol. Chem.* **1984**, *259*, 3368−3374.
(75) Fisher, M. T. Differences in Thermal Stability between Reduced and Oxidized Cytochrome b_{562} from *Escherichia coli*. *Biochemistry* **1991**, *30*, 10012−10018.
(76) Wolynes, P. G. Symmetry and the Energy Landscapes of Biomolecules. *Proc. Natl. Acad. Sci. U.S.A.* **1996**, *93*, 14249−14255.

AR970078T